Melting Stage Analysis for Indirect Freeze Desalination

by
Mason G. Pratt

A THESIS

submitted to

Oregon State University

Honors College

in partial fulfillment of
the requirements for the
degree of

Honors Bachelors of Science in Mechanical Engineering
Honors Associate

Presented June 5 2019
Commencement June 2019

AN ABSTRACT OF THE THESIS OF

Mason G. Pratt for the degree of Honors Baccalaureate of Science in Mechanical Engineering presented on June 5 2019

Title: Melting Stage Analysis for Indirect Freeze Desalination

Abstract Approved: _____
Deborah V. Pence

To investigate the melting stage of indirect freeze desalination three numerical models were developed. A zeroth, first, and second order analyses modeled the melting of ice around the outside of a pipe as a function of time. The zeroth order analysis assumes the system to be steady state. The first order analysis allows for variations in time and assumes the temperature profile along the pipe to be linear. The second order analysis allows for variations in time and space and considers the full length of the pipe. These models use water as the working (heating) fluid and were run at a base case consisting of inlet temperature of 293 K, mass flow rate of 0.1 kg/s, pipe inner radius of 3.85 mm and pipe outer radius of 4.95 mm. The effect of varying parameters on the output volume of water was investigated by running the second order analysis, changing one parameter at a time relative to the base case conditions. Increases in inlet temperature and mass

flow rate yielded increases in output volume. Increasing mass flow rate above 0.1 kg/s had no benefit on the output volume. Decreases in inner and outer pipe radii resulted in additional output volume. Smaller pipe radii worked better because many small pipes have more surface area than fewer large pipes. Using the second order analysis with a similar analysis of the freezing stage, the optimal cycle time of 68.2 minutes was found to produce 12.3 liters of fresh water per tube per day at the cost of 22.5 kWh/liter.

Key Words: Desalination, Freezing, Indirect, Melting

Corresponding E-mail Address: prattma@oregonstate.edu

Melting Stage Analysis for Indirect Freeze Desalination

by
Mason G. Pratt

A THESIS

submitted to

Oregon State University

Honors College

in partial fulfillment of
the requirements for the
degree of

Honors Bachelors of Science in Mechanical Engineering
Honors Associate

Presented June 5 2019
Commencement June 2019

Honors Baccalaureate of Science in Mechanical Engineering thesis of Mason G. Pratt presented on June 5 2019

APPROVED:

Deborah V. Pence
Mentor, representing Thermal-Fluid Sciences

James Liburdy
Committee Member, representing Thermal-Fluid Sciences

Joshua Gess
Committee Member, representing Thermal-Fluid Sciences

Toni Doolen
Dean, Oregon State University Honors College

I understand that my thesis will become part of the permanent collection of Oregon State University libraries. My signature below authorizes release of my thesis to any reader upon request.

Mason G. Pratt, Author

ACKNOWLEDGEMENTS

Thank you to my advisor Dr. Deborah Pence for your unwavering support during the thesis process. From start to finish your guidance and wisdom proved to be invaluable. I appreciate not only your help with the final product but the motivation you gave me to reach the finish line.

Thank you to my closest friends Josh Cook, Francisco Boschetti and Trevor Whitaker. All three of you helped me keep my work in the context of the overall project. For the hours you all spent helping me with coding, writing, or trying to stay sane, thank you.

Thank you to my fiancee Claire Pflieger for being there for me every hour of every day. You know my limits better than I do, and push me to be the very best I can. This thesis would not have been possible without your love and support

Thank you to all of my friends and family who have helped me get to this point. I would not be the person I am without your guidance. I am indebted to each one of you!

TABLE OF CONTENTS

LIST OF FIGURES

LIST OF TABLES

NOMENCLATURE

Symbols

Δt	Time step $\left[s\right]$
Δz	Spatial step $\left[m\right]$
$\dot{m}$	Mass flow rate $\left[\frac{kg}{s}\right]$
λ	Enthalpy phase change for water/ice $\left[\frac{J}{kg}\right]$
ρ	Density $\left[\frac{kg}{m^3}\right]$
c	Specific heat $\left[\frac{J}{kg \cdot s}\right]$
E	Energy $\left[J\right]$
h	Heat transfer coefficient $\left[\frac{W}{m^2 \cdot °C}\right]$
k	Thermal conductivity $\left[\frac{W}{m \cdot °C}\right]$
L	Length $\left[m\right]$
R	Thermal resistance $\left[\frac{°C}{W}\right]$
r	Radius $\left[m\right]$
T	Temperature $\left[°\mathrm{C}\right]$
t	Time $\left[s\right]$
U	Internal energy $\left[J\right]$
V	Volume $\left[m^3\right]$

Subscripts

$_{adv}$	Advection

$_{avg}$ Calculated average property between axial spatial steps

$_{A}$ Inner surface pipe wall

$_{B}$ Outer surface pipe wall

$_{cond}$ Conduction

$_{conv}$ Convection

$_{C}$ Inner surface of ice

$_{D}$ Outer surface of ice

$_{ice}$ Pure ice

$_{in}$ Pipe inlet (for working fluid)

$_{i}$ Length increment i

$_{out}$ Pipe outlet (for working fluid)

$_{pc}$ Fresh water phase change region

$_{pipe}$ Pipe

$_{sl}$ Phase change for fresh water between solid/liquid phases

$_{water}$ Fresh water

$_{wf}$ System working fluid (heating fluid)

Superscripts

^{k} Time step k

1 INTRODUCTION

1.1 Fresh Water Needs

Access to clean water is critical for all life on earth. Humans rely on water not only for consumption, but also to produce most sources of food. Most of the water on earth is salt water, which is not useable for drinking or food-related applications. Fresh water makes up just 2.53% of water on the planet, and less than one third of that is accessible by humans [1]. As a result, the production of fresh water is critical to supporting human populations across the globe. In drought-prone areas, access to fresh water can be problematic.

California has an enormous demand for fresh water, which is used to support large population centers, wildlife, and many acres of agriculture. Fresh water can be scarce, especially in the arid summer months. In certain parts of California, much of the fresh water is collected from underground aquifers. These aquifers act as natural wells that slowly fill with fresh water. However, many of these fresh water aquifers are filling with salt water. This is caused primarily by irrigation runoff carrying contamination from agriculture products and draining the aquifers to an abnormally low level [2]. Under special circumstances these salty aquifers can return to their fresh state, but most of them cannot [2]. Humans can taste the salt in water at approximately 150 ppm [3], and the salty aquifers often exceed 500 ppm [4]. Grapes and strawberries, two of California's largest agriculture products, cannot tolerate salt above 25 and 8 ppm, respectively [5]. For the salty aquifers, the

salt water can still be collected but must be desalinated. Because there is a need for more fresh water in these areas and most salty aquifers cannot be used, developing a desalination system to make fresh water directly from the salty aquifers is a very promising option. Portable fresh water solutions would be advantageous over large permanent desalination plants because they can be relocated or removed as needed with lower capital investment. In addition to the salty aquifers, a portable desalination system could also be used during disaster relief to ensure everyone has access to drinkable water.

1.2 Scope of Analysis

The analyses covered in this paper investigate the melting stage for an indirect freeze desalination system. The freezing stage was studied simultaneously by Whitaker [6], and is not included in this publication. The melting analysis consists of three separate models: a zeroth order steady state control volume analysis, a first order time variant control volume analysis, and a second order time and space variant control volume analysis. The three analyses demonstrate how much fresh water can be melted by the system in question. These analyses can be used to simulate many different operation conditions to understand the relationships between the output volume of fresh water and variables such as the mass flow rate of the working fluid, inlet temperature of the working fluid, and pipe inner and outer radii.

1.3 Project Goals

The goal of this project is to develop a computer-based numerical model for the melting stage of an indirect tube-in-tank freeze desalination system. The intention of the model is not that it can give the exact behavior of the system under optimal conditions, but that the model can give an approximation of what the output may look like. This can be used to determine whether such a system could be viable in the future. The results of this analysis can help decide whether or not future research on the topic should be conducted.

2 BACKGROUND

2.1 Types of Desalination

Desalination technologies can be split into three main subgroups: pressure-based, thermal-based, and chemical-based [7]. The pressure-based technologies use a pressure difference to force feed water through semi-permeable membranes that capture the salt but allow the fresh water to flow through freely. Pressure-based systems almost always run in one continuous cycle because there is only one step in the desalination process. The thermal-based technologies directly change the temperature of the salt water, known as feed water, to cause a phase change which separates the salt from the fresh water. Thermal methods are typically run in batches because there are several distinct processes that must be run in order to create fresh water. The chemical-based technologies use chemical reactions to precipitate the salt out of the solution.

2.1.1 Reverse Osmosis Desalination

Reverse osmosis (RO) is the most popular desalination technology. It is a pressure-based method that uses high pressure to push the feed water through semi-permeable membranes. These membranes allow water to pass through but catch and reject salts. It is important to note that RO functions much better for lower salinity feed water. This is because the osmotic pressure to pass through the membranes increases with the salt concentration of the water [8]. For this reason,

RO technology usually makes a distinction between brackish and seawater RO. Brackish water has a lower salt concentration than seawater, so it uses much less energy. Seawater RO systems are only able to recover 35-40% of the feed water volume for high salinity water [8]. Brackish RO plants use approximately 9 kJ to produce each kilogram of product water, while seawater RO systems use 23 kJ [9]. One of the biggest issues with RO is that over time the membranes experience fouling and must be replaced. The cost of materials for each membrane and the need to frequently replace membranes causes down time which results in increased costs while hurting productivity. As a result, the filters are kept clean as long as possible through extensive pretreatment of the feed water. Pretreatment filters out the vast majority of impurity from the feed water including sand and large particulates, microorganisms, and unhealthy natural compounds [8]. Depending on which chemicals are used, posttreatment of the product water can be required as well.

2.1.2 Electrodialysis Desalination

Electrodialysis (ED) desalination is a pressure-based system that uses electricity to pull charged particles out of the feed water. An anode and cathode are placed on either side of the feed water stream. The anode and cathode attract negative and positive charges, respectively. Semi-permeable membranes are placed between the feed water and each electrode which allow water to pass through but stop charged particles. When a DC voltage is applied across the anode and cath-

ode any charged particles in the water are attracted, which are then trapped by the membranes. Because salt is made of positively charged sodium ions and negatively charged chlorine ions, both are pulled out of the water and captured. Because ED does not have to change the temperature of the feed water it uses very little energy. Typical ED applications use 2.6 kJ per kilogram of water [9]. However, ED struggles with highly concentrated feed water due to membrane limitations [10]. Because ED can only remove ionic compounds it must go through pretreatment thoroughly to avoid any non-charged contaminants. The product water often requires some level of posttreatment as well.

2.1.3 Multi-Stage Flash Desalination

Multi-stage flash (MSF) is one of the most common desalination type in the world [9]. MSF uses thermal energy to evaporate the feed water. First, the feed water is heated to the operating temperatures, typically 90-120°C [11]. The feed water then enters a low pressure chamber. Due to the low pressure the boiling point of the feed water is dramatically decreased, causing a small portion of it to rapidly evaporate into water vapor. This process is called flashing. MSF typically uses a technique called staging which means the feed water is run through many of these low pressure flash chambers in series. Each stage is at a slightly lower pressure than the previous to counteract the additional salt concentration [11]. Over the course of 20+ stages the feed water incrementally evaporates until very little is left. When the feed water evaporates the salt is left behind, meaning

the water vapor is made up entirely of fresh water. This water vapor is then condensed into product water. Preheating the feed water and controlling the pressure of many different flash chambers can be very energy intensive. However, many techniques have been developed to improve energy efficiency. MSF plants are often coupled with power plants to take advantage of the power plant's waste heat for the preheating. Additionally, during condensation heat is released which can be captured and used for preheating. MSF plants use approximately 265 kJ to produce 1 kg of product water [9], much more than competing technologies. MSF makes up for this by running very quickly and simply. It is very resistant to scaling when additives are used in the feed water [11]. Due to the inherent staging, MSF can be effectively used in small and large scale applications.

2.1.4 Vapor Compression Desalination

Vapor compression (VC) desalination systems evaporate the feed water using compressed steam. First the feed water is compressed, increasing its pressure and temperature. This compression can be accomplished using a mechanical compressor or using thermal energy. This subtle difference is what divides mechanical vapor compression (MVC) from thermal vapor compression (TVC). The pressurized feed water is then fed into an evaporator causing the formation of water vapor. This water vapor is pulled out and condensed into product water. Many techniques can be employed in VC to increase thermal efficiency. One technique that only applies to TVC is staging during evaporation which allows some vapor

to be created using less compression [9]. Another method is to use the product vapor and water to heat the feed water. VC tends to be used in small to medium scale applications because it is relatively simple and energy efficient. VC plants typically use 31 kJ to produce each kilogram of water [9].

2.1.5 Freezing-Melting Desalination

Freezing-Melting desalination (FM), also known as freeze desalination systems, create fresh water by making pure ice and then melting it. During the freezing process the ice crystals formed are made of pure water molecules and impurities are left in the liquid solution. Partially freezing salt water results in pure ice and a more concentrated brine. After discarding the brine the resulting ice is melted to produce product water. This process is very energy efficient when compared to other methods. From a starting salt water temperature of 25 °Celsius it takes six times as much energy to heat and then vaporize the water as it does to cool and then freeze it [12]. Because freeze desalination systems operate at low temperatures, scaling and corrosion are much less problematic. Freeze desalination does have several drawbacks from more conventional methods. First, it can be difficult to manage the ice in a desalination system. It cannot be transported or handled as easily as the water vapor in other systems, so careful considerations must be taken in the design and geometry of any freeze desalination system. Second, separating the ice from the brine can be difficult in some applications. Most of the separation can be done by simply draining away the brine, but not all of it.

Because freezing does not happen uniformly or instantly, at any boundary between the ice and brine a two-phase mixture is left which contains salt. This layer does not drain away with the water and must be separated another way. This can be accomplished by washing the ice with clean water [13].

2.1.6 Desalination Method Comparison

The ideal desalination method has a high energy efficiency, high fresh water output, low risk of scaling or corrosion, low level of maintenance and no required pretreatment or posttreatment. Table 1 shows the different strengths and weaknesses of the discussed methods for desalination.

Table 1: Comparison of Different Desalination Methods [6]

	MSF	**RO**	**VC**	**ED**	**FM**
Energy Efficiency	Low	High	Moderate	High	High
Required Pre/Posttreatment	No	Yes	No	Yes	No
Risk of Fouling	No	Yes	No	Yes	No
Risk of Corrosion	Yes	No	Yes	No	No
Required Wash Process	No	No	No	No	Yes

For the application of this research freeze desalination was chosen due to its high energy efficiency and low risk of fouling and corrosion. This stems from its low operation temperature. Freeze desalination requires washing and draining of the brine, but these complexities are not prohibitive to overall design.

2.2 Detailed Freeze Desalination

Rudimentary freeze desalination was historically used by sailors to create, store or harvest fresh water while at sea. The first scientific experiments with freeze desalination were conducted in the late eighteenth century. There was very little research done on the topic from this point until the middle of the twentieth century. Scientists began experimenting with different styles, setups, and designs to better understand the process [14]. Freeze desalination can be split into two subgroups of direct and indirect freeze desalination based on the method of freezing.

2.2.1 Direct Freeze Desalination

Direct freeze desalination means the cold refrigerant is directly contacting the salt water. This is typically done by spraying the refrigerant through a nozzle to directly contact and cool the salt water. The refrigerant is pressurized sufficiently that it leaves the nozzle as a liquid. It then travels through the nozzle and boils due to the decreased pressure. This vaporization absorbs heat energy from the surrounding salt water and causes the formation of small ice crystals [15]. These small ice crystals are then grown larger with time. Because the salt water and refrigerant contact, the choice of refrigerant must meet a multitude of criteria. The refrigerant must:

- Be nontoxic
- Have a boiling point below the freezing point of water

- Not mix or react with water
- Not absorb water

In addition, the ideal refrigerant would be easily available and cheap, but these are not requirements. Fluids such as butane, carbon dioxide, and liquified natural gas have all been used in previous applications [16].

Ice formation in direct freeze desalination can be conducted in batches or continuously. Once the ice crystals are of sufficient size, they can be removed from the freezing area and washed. This eliminates the salt slurry layer at the expense of some of the product water that was frozen. Because there is so much surface area on the ice crystals the washing process tends to be more important and more complex than for indirect freeze desalination. Improvements made for the washing process may dramatically reduce the volume of water used for washing as well as increase the output volume of product water due to less wasted ice.

2.2.2 Indirect Freeze Desalination

Indirect freeze desalination is any process where the refrigerant does not contact the salt water. This typically means that some form of solid is used between the two fluids as in a heat exchanger. This intermediate material adds thermal resistance to the heat transfer which increases the energy cost for freezing when compared to direct methods. However, it opens up the use of many more refrigerants with more desirable thermal properties.

Indirect freeze desalination cannot operate continuously and must be conducted in batches. The ice crystals formed by indirect methods are usually larger than those using direct methods due to the constraint of batching. This introduces the issue of stirring for indirect methods. Because the salt is separated at the point of freezing, an area of high salt concentration forms at the brine-ice interface. This high concentration decreases the freezing temperature and causes less ice to form [17]. This can be counteracted by stirring the feed water to uniformly distribute the salt. The concentration of the feed water will still increase but its effects will be much less drastic.

Indirect freeze desalination systems cover a wide variety of complexities. The simplest involve an ice mass that does not move and contacts a heat exchanger. This keeps system complexity to a minimum, but stirring and the slurry layer are both issues in this case. Using a more complex design, some systems rotate the ice on a drum, serving to both stir the feed water and clear away some of the slurry layer. A knife attachment can be placed such that the ice can be rotated and slurry scraped off by the knife [15]. Other methods include vacuum freezing where the refrigerant is vaporized with a vacuum to cool the feed water and falling-film where a thin film of feed water runs over the heat exchanger.

2.3 Related Work

The research in this paper is solely focused on the melting stage of indirect freeze desalination. This work alone is not enough to fully evaluate a freeze desali-

nation system. Two theses were simultaneously conducted alongside this one to investigate the entire system. The first is a counterpart which analyzes the freezing stage of desalination using similar methodology to this one [6]. The freezing and melting analyses together can run simulations of the full cycle. This is important for further work on the topic of optimization and improvements. The second thesis covers the design of the system and conducts a reliability analysis [18]. This work served to inform and evaluate the system's design as well as highlight specific areas for further improvement.

3 METHODOLOGY

The system investigated in these analyses is an indirect tube freeze desalination system which consists of a single pipe positioned vertically through a tank. During the freezing portion of desalination ice is built up on the outside of this pipe. During the melting portion of desalination ice is melted by flowing a warm working fluid through the pipe. All analyses presented are related only to the melting process. Figure 1 details the system geometry in cross section.

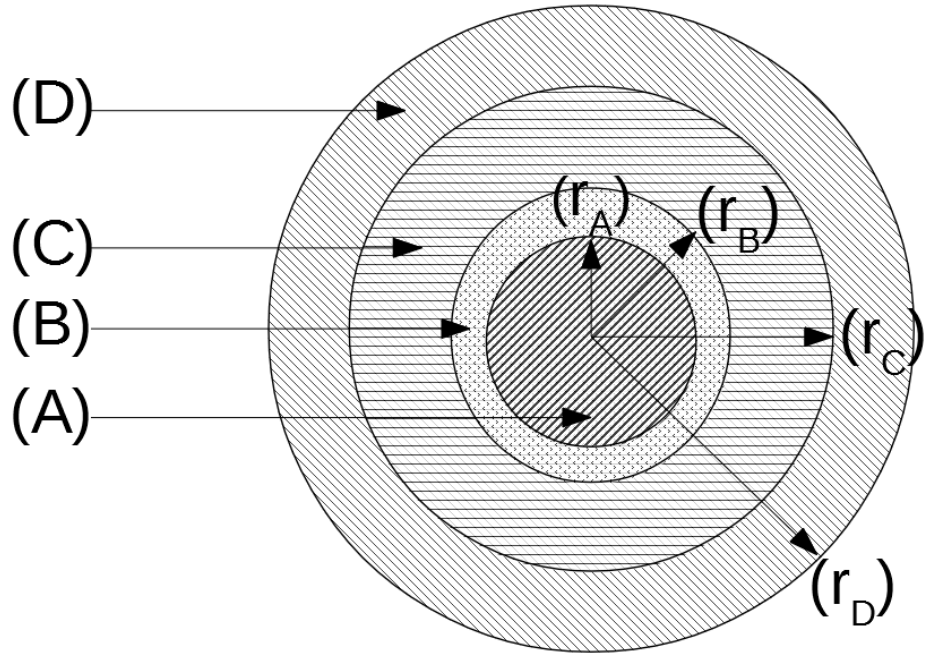

Figure 1: Melting Chamber Model, Vertical View

Region A is the working fluid. It is heated by an outside source and then flowed through the center of the ice-covered pipe. For these analyses the working

fluid was chosen to be fresh water due to its very high specific heat capacity. All of the heat that melts the ice during operation comes from this hot water.

Region B is the pipe material. This was chosen to be stainless steel due to its corrosion resistance in the presence of salt water. The heat from the hot water in the center of the pipe is transferred through the pipe wall via conduction to the ice.

Region C is the fresh water produced from melted ice. This region grows larger during system operation. This water is heated via natural convection at the pipe wall. Energy flows through the water to the ice/water interface separating regions C and D. As the melting portion of the desalination process progresses region C grows until all ice has been melted.

Region D is the ice that has not yet been melted. The ice/water interface absorbs heat from the water in region C and melts. When the desalination process is complete, region D will be nonexistent.

3.1 Zeroth Order Analysis

The zeroth order analysis idealizes the system as steady state. Due to this simplification, it is the least accurate of the three analyses. It demonstrates the ideal fresh water output of the system. This analysis is solved using only one

equation. Derivation of this equation starts with the energy balance of the whole system. Applied to the control volume in Figure 2,

$$\frac{dE}{dt} = \dot{Q} - \dot{W} + \dot{m}_{in}h_{in} + \dot{m}_{out}h_{out} \tag{1}$$

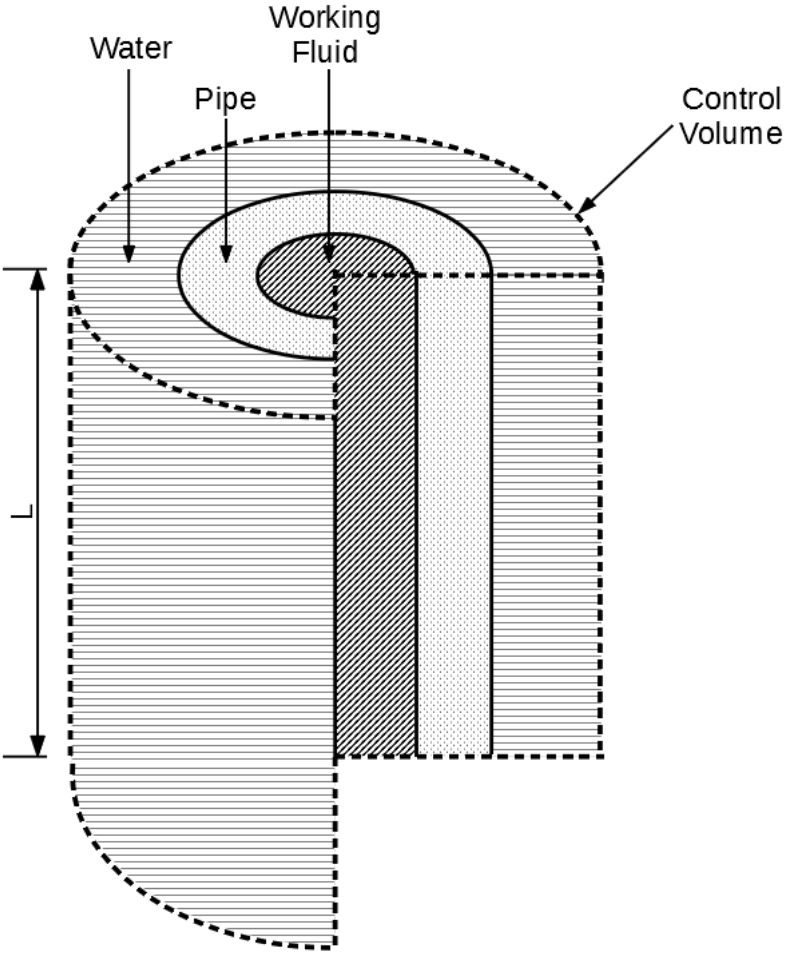

Figure 2: Control Volume #1

where $\dot{m}_{in}$ and $\dot{m}_{out}$ are the mass flow rates of the working fluid in and out of the system respectively. By conservation of mass $\dot{m}_{in} = \dot{m}_{out} = \dot{m}_{wf}$. Because the system is assumed to be steady state, $\frac{dE}{dt} = 0$. Because the working fluid is

considered to be incompressible h_{in} and h_{out} can be replaced using $\Delta h = c\Delta T$. These substitutions yield

$$\dot{Q} = \dot{m}_{wf} c_{wf} (T_{out} - T_{in})_{wf} \tag{2}$$

For the zeroth order analysis T_{out} and T_{in} are both fixed. Because the right side of Equation 2 is constant, $\dot{Q}$ must also be constant. This means that for this analysis, $\dot{Q}$ is not a function of the changing thermal resistance of convection through the water. Because $T_{out_{wf}} < T_{in_{wf}}$, $\dot{Q}$ must be a negative quantity and equal to

$$\dot{Q}_{pc} = \frac{-\Delta V_{water}}{\Delta t} \rho \lambda_{sf} \tag{3}$$

Substituting this expression for $\dot{Q}$ in Equation 2 and changing appropriate signs then solving for ΔV_{water} yields

$$\Delta V_{water} = \frac{\dot{m}_{wf} c_{wf} (T_{in} - T_{out})_{wf}}{\rho_{water} \lambda_{sf}} \Delta t \tag{4}$$

After inputting a given time step for Δt, all terms in Equation 4 are known and ΔV_{water} can be directly solved to yield the volume of water melted during that time step. By increasing the time step the relationship between the elapsed time and volume of melted water ΔV_{water} can be observed. For this analysis, $\Delta V_{water} = V_{water}$ because the melted volume is zero at the initial state. Large time steps are not a problem because the system is at steady state.

3.2 First Order Analysis

In reality as the water region grows the thermal resistance of convection through the water increases and reduces $\dot{Q}_{pc}$ thereby slowing the melting process. In addition the outlet temperature of the working fluid, $T_{out_{wf}}$, will vary. The first order analysis breaks the system into discrete time steps to better understand how the system changes as a function of time. The first order analysis control volume in Figure 2 is used to simultaneously solve four linear equations at each time step to yield the volume of water melted over that time step.

The first equation is an energy balance of the working fluid.

$$\frac{dE}{dt} = \dot{Q} + \dot{m}_{wf} c_{wf} (T_{in}^{k} - T_{out}^{k})_{wf} \tag{5}$$

This analysis is not steady state so $\frac{dE}{dt}$ is equal to the sum of the rate of changes of internal, potential, and kinetic energy.

$$\frac{dE}{dt} = \frac{d(KE)}{dt} + \frac{d(PE)}{dt} + \frac{dU}{dt} \tag{6}$$

For this analysis the changes in potential and kinetic energy are neglected, leaving only the internal energy term. This can be expanded into distinct terms for the internal energy of the pipe, working fluid, and water.

$$\frac{dU}{dt} = \frac{d}{dt}(m_{pipe} u_{pipe}) + \frac{d}{dt}(m_{wf} u_{wf}) + \frac{d}{dt}(m_{water} u_{water})) \tag{7}$$

The relative magnitudes of these terms are drastically different. The mass of the pipe does not change at, and the internal energy changes very little, so the energy term of the pipe is neglected. The rates of change of mass for the water is on the order of 10^{-5} while the rate of change of mass for the working fluid is on the order of 10^{-3}. Because the working fluid term is so much larger it dominates Equation 7 and the effect of the water term is negligible. This leaves only the working fluid term to equal the change in internal energy. Because the working fluid is incompressible the following relation can be used:

$$\frac{du_{wf}}{dt} = c_{wf}\frac{dT_{wf}}{dt} \tag{8}$$

The rate of change of working fluid temperature can be simplified using forward finite difference approximation:

$$\frac{dT_{wf}}{dt} = \frac{(T^k - T^{k-1})_{wf}}{\Delta t} \tag{9}$$

Using Equations 8 and 9 for the value of $\frac{dE}{dt}$ in Equation 5 yields

$$m_{wf}c_{wf}\frac{(T^k - T^{k-1})_{wf}}{\Delta t} = \dot{Q}^k + \dot{m}_{wf}c_{wf}(T^k_{in} - T^k_{out})_{wf} \tag{10}$$

The second equation comes from approximating the working fluid temperature profile axially through the pipe as linear. An average temperature can be represented by

$$T^k_{wf_{avg}} = \frac{(T^k_{in} + T^k_{out})_{wf}}{2} \tag{11}$$

Recall that $\dot{Q}^k$ in Equation 10 will yield a negative quantity, thus all equations for $\dot{Q}^k$ must yield a consistent sign. Therefore, the third equation comes from using a thermal resistance analogy from the working fluid in region A to the ice/water interface at the outer boundary of region C.

$$\dot{Q}^k = \frac{T_C - T_A}{\Sigma R} \tag{12}$$

Because T_A is the temperature of the working fluid, it can be replaced with the expression in Equation 11. The temperature at the water/ice boundary is T_C, which is known to be equal to T_{pc} the temperature of phase change. Due to the system's concentric design, all of the thermal resistances are added in series, so $\Sigma R = R_{wf} + R_{pipe} + R_{water}$. Thus Equation 12 can be rewritten as

$$\dot{Q}^k = \frac{T_{pc} - T^k_{wf_{avg}}}{R_{wf} + R_{pipe} + R_{water}} \tag{13}$$

The individual resistances are as follows:

The thermal resistance of convection of the working fluid is

$$R_{wf} = R_{convection} = \frac{1}{h_{wf} A_A} \tag{14}$$

where $A_A = 2\pi r_A L$, the surface area of the contact region between the working fluid and the pipe wall. The convective heat transfer coefficient h_{wf} is calculated from the Nusselt number which comes from the Dittus-Boelter equation:

$$Nu_D = 0.023 Re_D^{0.8} Pr^n \tag{15}$$

where Pr is the Prandtl number and $n = 0.3$ because the working fluid is being cooled. This equation is valid for $0.7 \leq Pr \leq 160$, $Re_D \geq 10000$, and $\frac{L}{D} > 10$. Using this Nusselt number, h_{wf} is

$$h_{wf} = \frac{Nuk_{wf}}{D} \tag{16}$$

where D is the inner diameter of the pipe. The thermal resistance of conduction through the pipe wall is

$$R_{pipe} = R_{conduction} = \frac{\ln\left(\frac{r_B}{r_A}\right)}{2\pi k_{pipe} L} \tag{17}$$

where k_{pipe} is the thermal conductivity of the pipe at temperature $T_{wf_{avg}}$.

The resistance of the melted water in the system can be handled three different ways. The first is to model the heat transfer as conduction through liquid water. For this case, the thermal resistance is

$$R_{water} = R_{conduction,water} = \frac{\ln\left(r_C/r_B\right)}{2\pi k_{water} L} \tag{18}$$

The second method is to model it as conduction through ice. This thermal resistance is

$$R_{water} = R_{conduction,ice} = \frac{\ln\left(r_C/r_B\right)}{2\pi k_{ice} L} \tag{19}$$

The third method is to model it as natural convection. The thermal resistance of natural convection can be approximated as conduction by calculating an equivalent thermal conductivity, k_{eff} [19]. This gives an equivalent thermal resistance of conduction as

$$R_{water} = R_{conduction} = \frac{\ln\left(r_C/r_B\right)}{2\pi k_{eff} L} \tag{20}$$

This k_{eff} value is calculated using the following correlation:

$$k_{eff} = 0.386 k_{water} \left(\frac{Pr}{0.861 + Pr}\right)^{\frac{1}{4}} Ra_c^{\frac{1}{4}} \tag{21}$$

In this equation Ra_c is the Rayleigh number for a cylinder, which is calculated from

$$Ra_c = \frac{g\beta}{\nu\alpha}(T_s - T_\infty)L_c^3 \tag{22}$$

where g is the acceleration due to gravity, β is the thermal expansion coefficient, ν is the kinematic viscosity, and α is the thermal diffusivity. All of these physical constants were evaluated at the average temperature of the melted water and are

assumed to be constant. For the melting chamber, $T_s = T_B$ and $T_\infty = T_C = T_{pc}$. The characteristic length, L_c in Equation 22, is calculated by the following expression:

$$L_c = \frac{2[\ln(r_C/r_B)]^{\frac{4}{3}}}{\left(r_B^{-\frac{3}{5}} + r_C^{-\frac{3}{5}}\right)^{\frac{5}{3}}} \tag{23}$$

Any of these three methods can be used to represent R_{water}. The differences between the models will be explored more in the Results section.

The fourth equation relates the phase change energy of the melting ice to the heat transfer into the ice

$$\dot{Q}^k = \frac{-\lambda_{sf}\rho_{water}\Delta V_{water}}{\Delta t} \tag{24}$$

where ΔV_{water} is the volume of water that is melted over the timestep Δt. Rewriting ΔV_{water} as a function of r_C using the geometry of an annulus this equation becomes

$$\dot{Q}^k = \frac{-\lambda_{sf}\rho_{water}\pi L[(r_C^{k+1})^2 - (r_C^k)^2]}{\Delta t} \tag{25}$$

While this equation is acceptable in this form, it is a function of $(r_C^k)^2$ which is not desirable. In order to solve this equation using matrices of linear equations it must be linearized, which is done using the approximation $r_C^k \approx r_C^{k+1}$, the nonlinear term

$(r_C^{k+1})^2 \approx r_C^k r_C^{k+1}$. This approximation is valid for small values of Δt. Equation 25 then yields

$$\dot{Q}^k = \frac{-\lambda_{sf}\rho_{water}\pi L r_C^k (r_C^{k+1} - r_C^k)}{\Delta t} \tag{26}$$

Equations 10, 11, 13 and 26 collectively have five unknowns; $\dot{Q}^k$, $T^k_{wf_{out}}$, $T^k_{wf_{avg}}$, Δt, and r_c^{k+1}. The four equations can be simultaneously solved in matrix form for each incremental Δt. This yields ΔV_{water}, the amount of water melted during timestep Δt. The ΔV_{water} can be added to the previously melted volume to determine the total melted volume of water using $V^{k+1}_{water} = V^k_{water} + \Delta V_{water}$. This yields the relationship for V_{water} versus t.

Let A be the following matrix:

$$A = \begin{bmatrix} 1 & \frac{m_{wf}c_{wf}}{\Delta t} & \dot{m}_{wf}c_{wf} & 0 \\ 1 & \frac{-1}{\Sigma R} & 0 & 0 \\ 0 & 2 & -1 & 0 \\ -\Delta t & 0 & 0 & \lambda_{sf}\rho_{water}\pi L r_C^k \end{bmatrix}$$

$$\begin{bmatrix} \dot{Q}^k \\ T^k_{wf_{avg}} \\ T^k_{wf_{out}} \\ r_C^{k+1} \end{bmatrix} = A^{-1} \begin{bmatrix} \dot{m}_{wf}c_{wf}T^k_{wf_{in}} + \frac{m_{wf}c_{wf}}{\Delta t}T^{k-1}_{wf_{avg}} \\ -\frac{T_{pc}}{\Sigma R} \\ T^k_{wf_{in}} \\ \lambda_{sf}\rho_w \pi L (r_C^k)^2 \end{bmatrix}$$

3.3 Second Order Analysis

The second order analysis is discretized in both time and space. The only difference between the first and second order analyses is that the second order splits the system into small subsections along its length, as seen in Figure 3. This is done to capture the effects of the working fluid's temperature drop along the length of the pipe for additional accuracy.

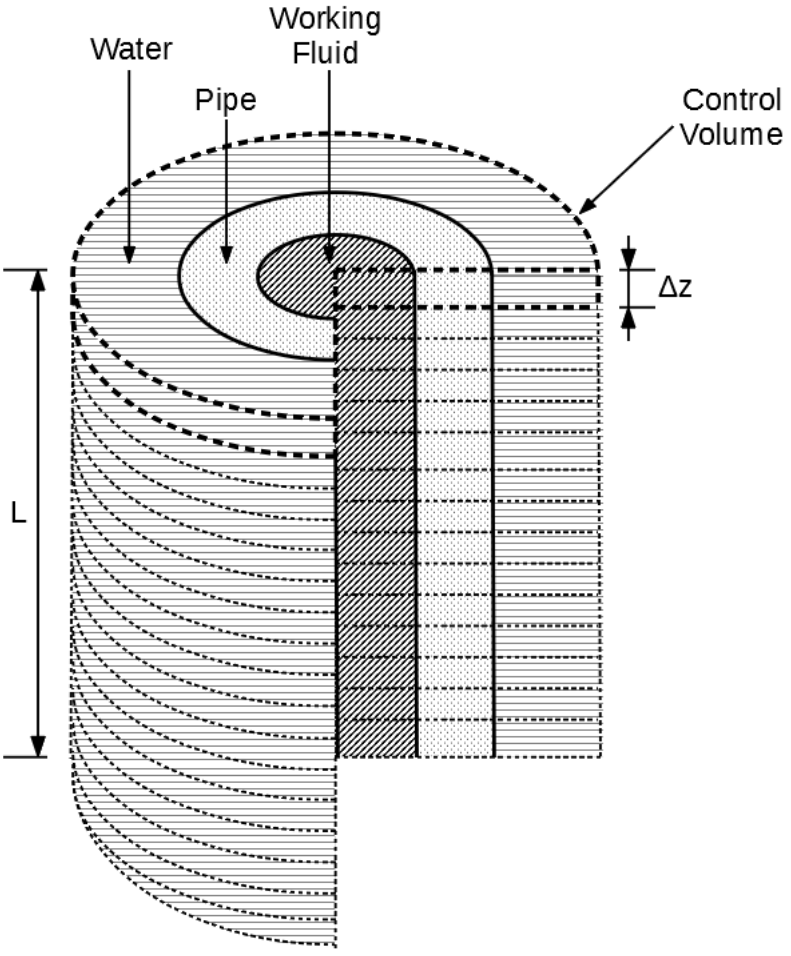

Figure 3: Control Volume #2

Due to the division of L into smaller spatial increments, there are two differences in the systems of equations for the first and second order analyses. The first change is that each length term L is replaced by a Δz term to limit the analysis to each individual spatial component.

The second change after the length is discretized is that $T_{wf_{in}}$ appears to be unknown for all but the first length step. However, it is known because $T_{wf_{in},i} = T_{wf_{out},i-1}$ where i represents the spatial location of the current control volume. Thus for each Δt the system of equations must also be solved at each length step starting at the inlet and moving to the outlet. By factoring in these two changes, the system of equations becomes

$$B = \begin{bmatrix} 1 & \frac{m_{wf}c_{wf}}{\Delta t} & \dot{m}_{wf}c_{wf} & 0 \\ 1 & \frac{-1}{\Sigma R} & 0 & 0 \\ 0 & 2 & -1 & 0 \\ -\Delta t & 0 & 0 & \lambda_{sf}\rho_{water}\pi\Delta z r_C^k \end{bmatrix}$$

$$\begin{bmatrix} \dot{Q}^k \\ T^k_{wf_{avg}} \\ T^k_{wf_{out}} \\ r_C^{k+1} \end{bmatrix} = B^{-1} \begin{bmatrix} \dot{m}_{wf}c_{wf}T^k_{wf_{in}} + \frac{m_{wf}c_{wf}}{\Delta t}T^{k-1}_{wf_{avg}} \\ -\frac{T_{pc}}{\Sigma R} \\ T^k_{wf_{in}} \\ \lambda_{sf}\rho_{water}\pi\Delta z (r_C^k)^2 \end{bmatrix}$$

Each time these matrices are solved, they yield the $\Delta V^k_{water_z}$ for the given Δt and Δz. For each timestep the spatial ΔV_{water_z} terms can be summed to find the

total change in volume over that period ΔV^k_{water}. The relationship between V_{water} and t is then determined using $V^{k+1}_{water} = V^k_{water} + \Delta V_{water}$.

4 RESULTS & DISCUSSION

4.1 Melting Stage Analysis

The zeroth, first, and second order analyses were conducted using a base case for geometric values and inlet temperature. These values are listed in Table 2. The value of each base case parameter was chosen by running the second order analysis many times and using a genetic algorithm to find the best combination of base case parameters. In order to keep the genetic algorithm from choosing overly large numbers each parameter was given an acceptable range and a maximum pump power was imposed. From the genetic algorithm output the mass flow rate and inlet temperature were increased to encourage a higher heat transfer rate and make trends more visible. The values for each base case parameter were held constant to compare the all three analyses. The effects of each parameter on the system are explored later in this section.

Table 2: Base Case Values

$\dot{m}_{wf}$ (kg/s)	L (m)	r_A (m)	r_B (m)	$T_{wf_{in}}$ (K)
0.1	0.67	0.00385	0.00495	293

Before the first and second order analyses can output accurate results, the time step and length step values had to be evaluated for convergence. This convergence testing ensured that the error due to these discretizations is low enough to provide accurate results. To conduct the convergence testing the second order

analysis was first run using relatively large values for the time and length steps (10 seconds and 0.5 m respectively). The time step was then halved and the simulation run again. After two sets of output a relative error was established between the two. The time step was again halved and the relative errors compared until the relative error was below 0.1%. This process was then repeated for the length step. When the relative error for both the time and length steps fell below 0.1% it was considered converged. Figure 4 shows the results of the convergence test. The final converged value for the time step was 0.0098 seconds and the converged length step was 0.0039 meters. With these values established the analyses were carried out.

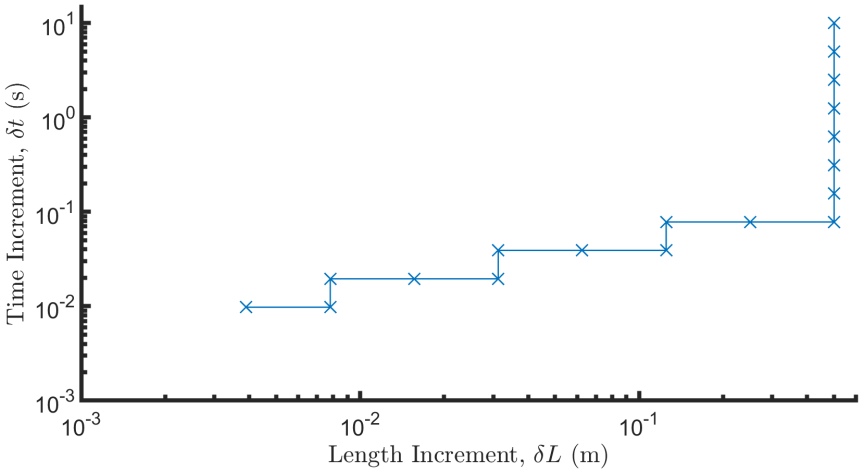

Figure 4: Convergence Test Results

The zeroth order analysis idealizes the system as steady state at the point of highest melting, meaning it yields the theoretical maximum values. It uses a fixed heat rate and assumes all heat goes into melting the ice. The volume of product

water produced over time is shown in Figure 5. The relationship is linear due to the fixed heat rate assumption for this analysis.

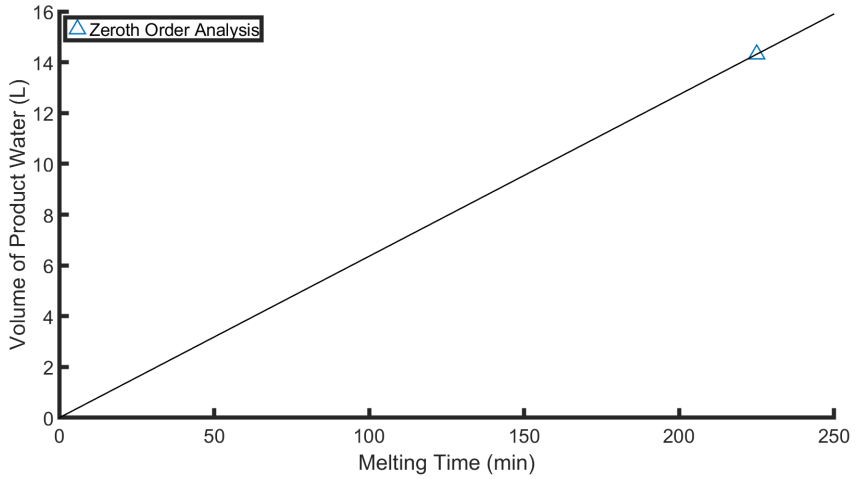

Figure 5: Zeroth Order Product Water Volume Versus Time

In reality, the melted water between the pipe wall and ice acts as a thermal insulator which decreases the rate of melting. Recall that there are three different methods to represent the thermal resistance of the melted water layer. These methods include conduction through water, conduction through ice, and the conduction analogy for natural convection. The only difference between the first two methods are the thermal conductivities between ice and water. The values used for k_{water} and k_{ice} in this analysis are 0.556 and 2.15, respectively. These two resistances and the volume of water they melt are compared in Figures 6 and 7, respectively. Ice has a higher thermal conductivity than water meaning ice will yield a smaller thermal resistance and produce more water. To make conservative estimates all values for total output of this system use the lowest yield method, which is conduction through water.

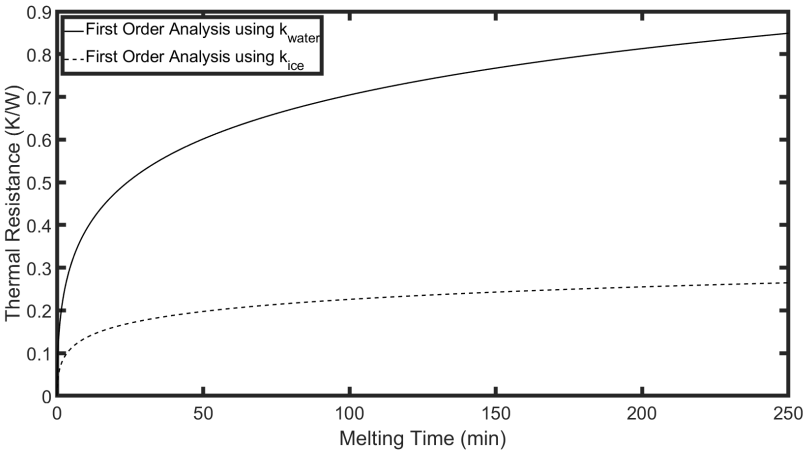

Figure 6: Resistance Comparison, Product Water R_{eff} Versus Time

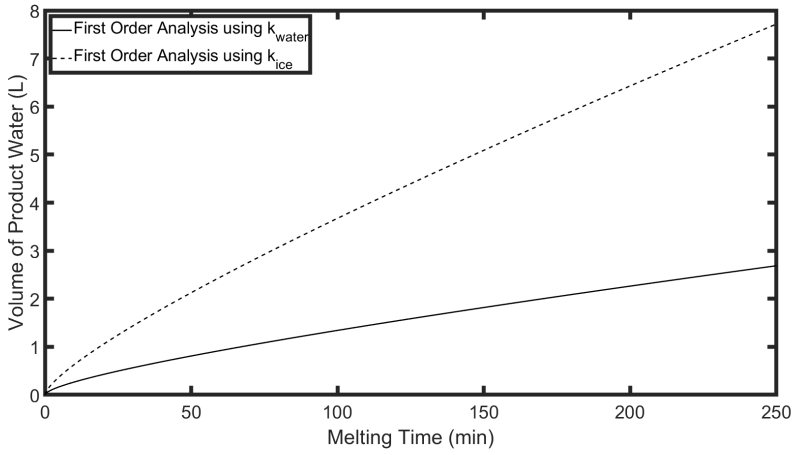

Figure 7: Resistance Comparison, Product Water Volume Versus Time

The third method to represent the thermal resistance of the water is natural convection. This can be done using a correlation to treat natural convection as conduction by calculating an effective thermal conductivity k_{eff}. This process is detailed in Section 3.2, Equations 20 - 23. One issue that arises with this approach is that unlike most substances, water has a negative thermal expansion coefficient below 297 K, as observed in Figure 8, which shows the relationship between temperature and thermal expansion coefficient of water. Water in the system must

be melted and warmed from 293 K, meaning it will certainly be in this temperature range for some period of time during operation. Having a negative thermal expansion coefficient results in a negative Rayleigh number. Using Equation 21 a negative Rayleigh number yields a complex number for k_{eff} because the Rayleigh number has an exponent of $\frac{1}{4}$. Thus even though this system fits in the stated constraints for the Prandtl and Grashof numbers, the correlation between natural convection and conduction is not applicable.

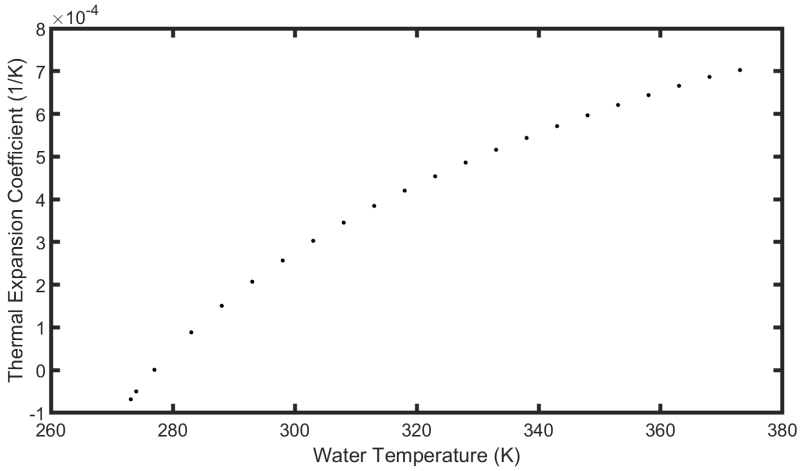

Figure 8: Thermal Expansion Coefficient of Water Versus Temperature

The first order analysis improves on the previous analysis by allowing the thermal resistance of the melted water to impact the rate of heat transfer. The volume of product water produced over time is shown in Figure 9.Recall that this analysis was run using the thermal conductivity of water because it has the lowest possible yield. The first order analysis is less linear than the zeroth order analysis because the thermal resistance of the melted water changes over time.

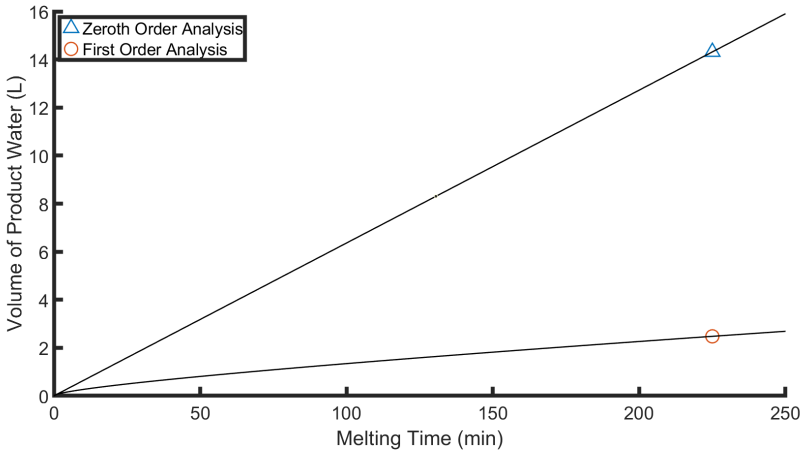

Figure 9: First Order Product Water Volume Versus Time

The second order analysis develops on the first order analysis by breaking the pipe length into smaller sections and conducting energy balances on each segment. The length of pipe was divided into fifty equal sections axially to capture the profile of the working fluid temperature. The volume of product water produced over time is shown in Figure 10. The first and second order results are nearly identical, meaning the working fluid temperature profile is nearly linear. This can be seen in Figures 11 and 12 which compare the approximated linear profile from the first order analysis and the actual temperature profile from the second order analysis. This matches expectations because for each energy balance the thermal conductivity of the pipe, specific heat of the working fluid, and convective heat transfer coefficient of the working fluid do not change.

Also observed from Figure 10 is that the volume production for the first and second order results taper off dramatically when compared to the zeroth order solution. This is due to the increasing influence that the resistance of the melted

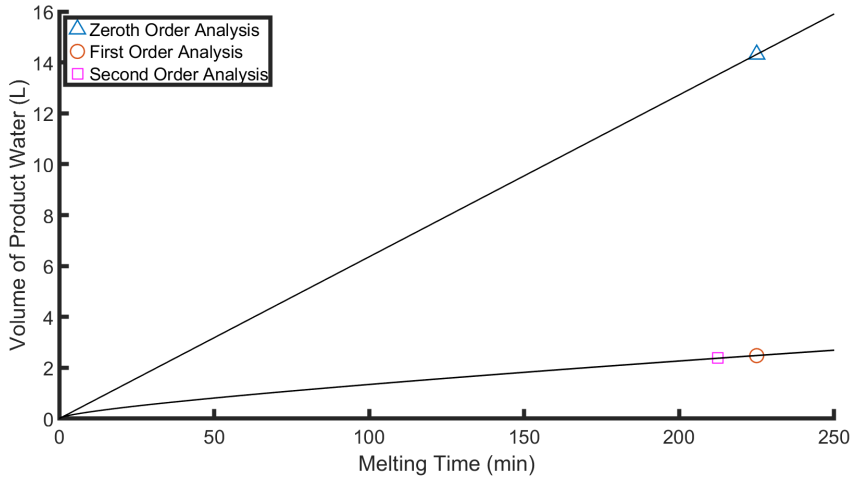

Figure 10: Second Order Product Water Volume Versus Time

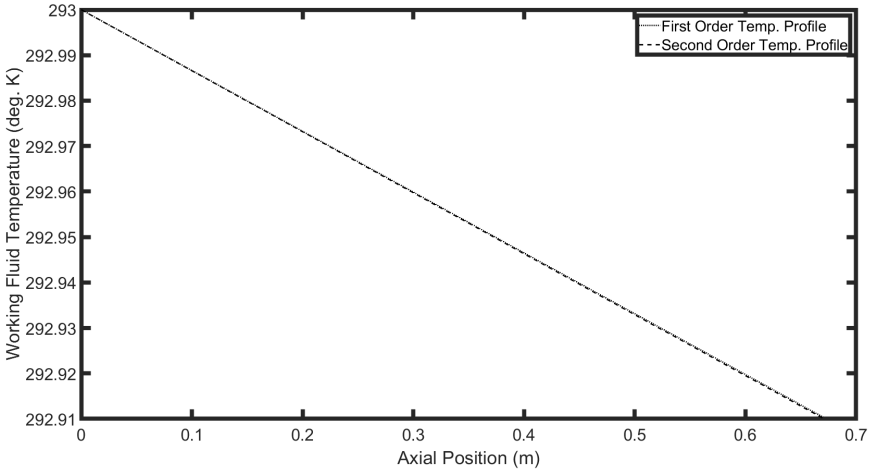

Figure 11: Temperature Profiles at 25 Minutes

water layer has over time. The resistance lowers the heat rate to the ice, and was not accounted for in the zeroth order analysis. However, the thermal resistance of conduction through the pipe and convection of the working fluid are significantly smaller than the resistance of the melted water. After only one second of operation the resistance of the melted water makes up 50% of the total resistance, and after eleven minutes it is the source of 95% of the total thermal resistance. The most

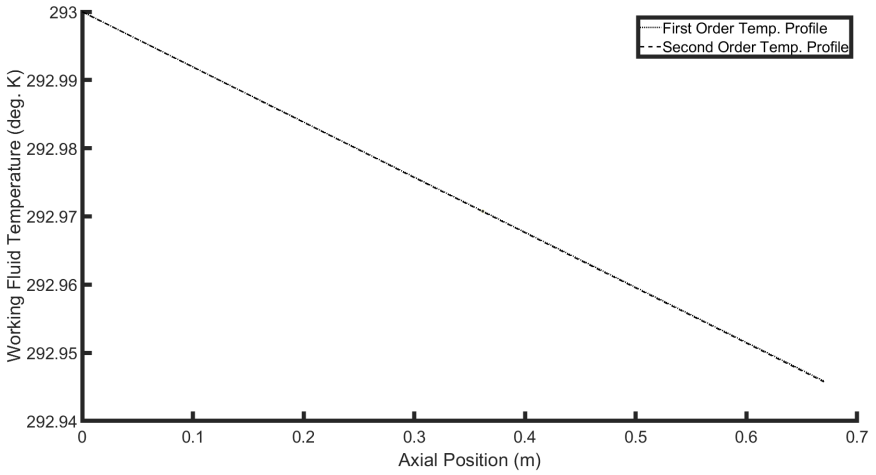

Figure 12: Temperature Profiles at 250 Minutes

water is melted when the total resistance is smallest, which is why the production of water slows down so significantly over time.

Although the base case values have been treated as constants thus far, they can be changed. Even small changes can have a noticeable impact on the system's performance. By changing the inlet temperature of the working fluid the rate of heat transfer, $\dot{Q}$, is altered. The inlet temperature individually does not have much meaning in the system of equations used. The inlet temperature influences the temperature difference between the working fluid and the melting ice, which directly controls the $\dot{Q}$. For this reason, as the temperature difference of the working fluid approaches zero it has more noticeable impacts on the system output. Figure 13 shows volume production versus time for a variety of different inlet temperatures. The inlet temperature has a larger effect on the volume when $T_{wf_{in}} - T_{pc}$ is closer to zero. As the inlet temperature increases so does the volume, though at the cost of larger heating requirements. The heater for the working fluid

must be able to match the $\dot{Q}$ of the system, which increases linearly with the inlet temperature.

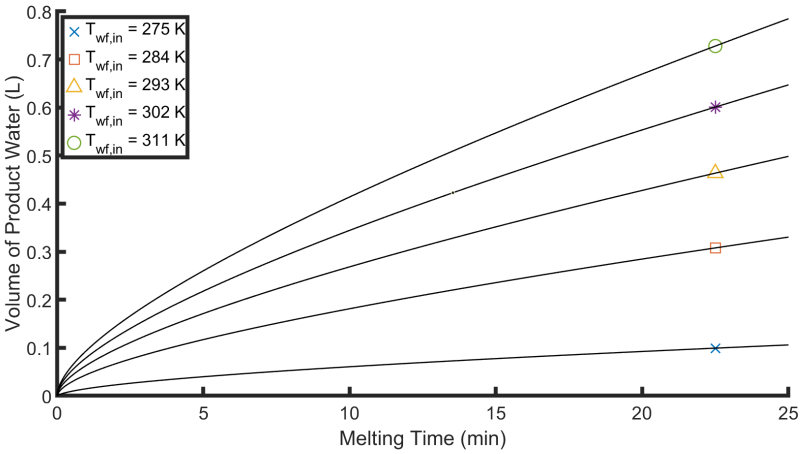

Figure 13: Effect of $T_{wf_{in}}$ on Product Water Volume Versus Time, with Pipe Size, Length, and Mass Flow Rate Held Constant

The mass flow rate describes the quantity of working fluid being pumped through the pipe each second. It is important in Equation 10 because it helps quantify the difference in the working fluid's thermal energy between the inlet and outlet. This difference affects the $\dot{Q}$ of the system. In general, higher mass flow rates result in higher $\dot{Q}$ values and higher volumes of product water. However, this relationship is not linear, as noted in Figure 14, which shows five different mass flow rates and their volume productions versus time. As the mass flow rate is increased each individual volume of fluid spends less time in the pipe. This means each volume of fluid has less time to transfer its heat to the pipe, and ultimately the ice, and the temperature difference between the inlet and outlet decreases. At a certain point the increase of mass flow rate and decrease of temperature difference nearly balance each other out, resulting in very little change to the overall water

production as observed in Figure 14. The lowest mass flow rate of 0.001 kg/s is the only outlier, above 0.01 kg/s the results are nearly indistinguishable. Higher mass flow rates require more powerful pumps and introduce higher pressure drops, so an ideal mass flow rate for this system would be in the range of 0.01 - 0.1 kg/s.

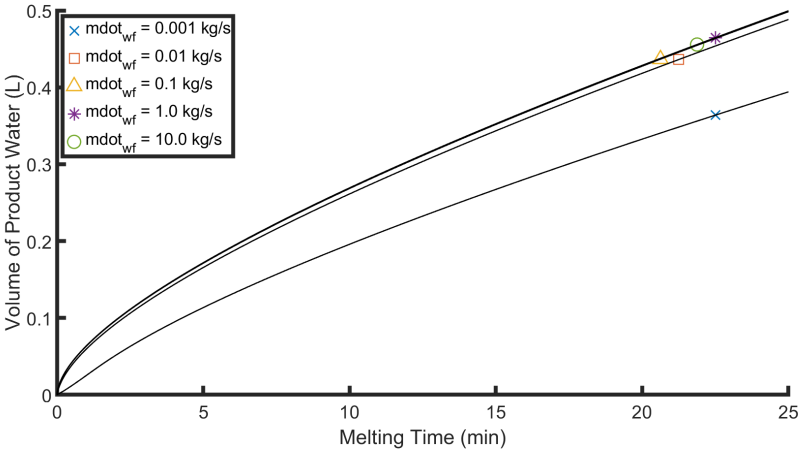

Figure 14: Effect of $\dot{m}_{wf}$ on Product Water Volume Versus Time, with Pipe Size, Inlet Temperature, and Length Held Constant

Changing the length of the system has a very straightforward impact on the output. Because there is very little variation axially due to the high mass flow rate at the base case, adding or subtracting from the length of the pipe is the same as scaling the output of product water. This is reinforced by the fact that mathematically in Equation 26 the heat transfer $\dot{Q}$ and L are related linearly. The power requirement for the pump also scales linearly with the length of the system. This can be observed by considering the pump power, which is calculated using

$$P = \rho \dot{V} g h_f \tag{27}$$

where P is the power, $\dot{V}$ is the volumetric flow rate, g is the gravitational constant, and h_f is the friction loss. The friction head is calculated using

$$h_f = f\frac{L}{d}\frac{v^2}{2g} \tag{28}$$

where f is the Darcy friction factor and v is the velocity. Substituting this relation in to Equation 27 gives a linear relation between L and pump power.The length of the pipe scales the volume production up or down linearly as long as an adequate pump is used. For very large lengths the pump requirement becomes prohibitively large which should be avoided.

The influence of the inner and outer radii of the pipe is not as intuitive at first glance. For this analysis both the inner and outer radii were varied simultaneously using commercially available pipe sizes. Increasing the inner radius will decrease the convection resistance of the working fluid and decrease the conduction resistance through the pipe. Increasing the outer radius will increase the conduction resistance through the pipe and decrease the resistance of the melted water. Because the analyses only use one pipe, larger pipes have a clear advantage over smaller pipes. They have more surface area to melt ice and exchange heat which allows them to produce more product water in the same amount of time. Comparing pipes one by one does not adequately capture the trade-offs between smaller and larger pipe radii. To compare them more equally the outputs of each different radii are compared using the number of pipes that could fit in a 100cm x 100cm square. The pipe spacing has been set in a grid pattern such that at

the end of a twenty-five minute cycle the melted water of each tube just touches its neighbors. Each pipe is assumed to have no effect on the heat transfer of its neighbors. The table below gives the inner and outer radii from five standard pipe sizes with the number of pipes that can fit in a 100cm x 100cm square.

Table 3: Pipe Size Chart

Pipe Number	r_A (mm)	r_B (mm)	Thickness (mm)	Pipes in 100 x 100cm
1	3.85	4.95	0.55	900
2	4.7	5.145	0.445	900
3	6.2	6.86	0.66	676
4	9.8	10.67	0.87	441
5	12.5	13.335	0.835	376

The thickness for each pipe varies which leads to different thermal resistances of conduction through the pipe for each case. These differences were taken into account during the analysis, but the contribution was negligible. The highest resistance through a pipe was on the order of 10^{-4}, which is equivalent to the thermal resistance of melted water after less than 0.05 seconds.

Figure 15 shows the output volumes over time for each pipe size. The general trend is that a setup using a greater number of small pipes outperforms a few large pipes. However, the second smallest pipe actually outperforms the smallest pipe. This is because they are so slightly different that the same number of pipes is used for either configuration. Because the larger of the two offers more surface area it is able to produce more product water.

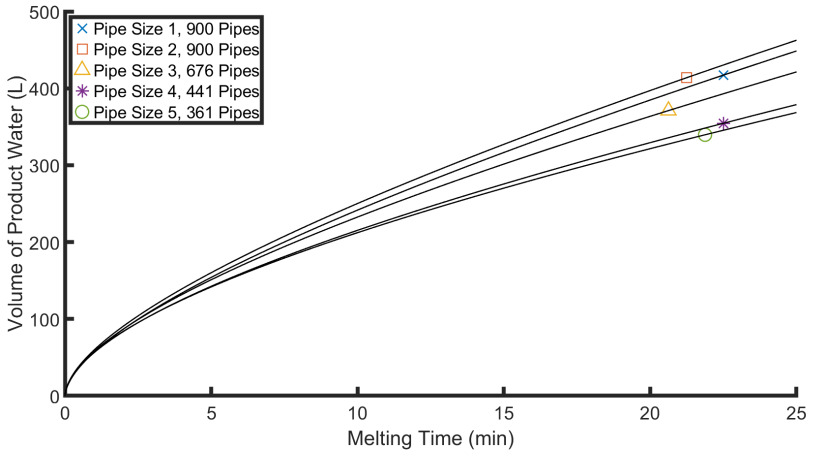

Figure 15: Effect of Pipe Size on Product Water Volume Versus Time, Using Varying Numbers of Pipes with Mass Flow Rate, Inlet Temperature, and Length Held Constant Per Tube

4.2 Overall Desalination System Analysis

The analysis conducted thus far only cover one stage of a freeze desalination system. The purpose of these analyses is ultimately to investigate the output of an entire freeze-thaw desalination system. Similar analyses were created and detailed for the freezing cycle [6]. When used in conjunction they are able to give predictions for the overall system output and assist in the design of a more optimal desalination system. The following analysis uses both sets of code to simulate the performance of an entire freeze-thaw desalination system.

It is important to determine how the volume production of the combined freezing and melting cycles over time. This amount of time is the cycle time τ_{cycle}, where $\tau_{cycle} = \Delta t_{freezing} + \Delta t_{melting} + \Delta t_{changeover}$. The value $\Delta t_{freezing}$ is the amount of time spent freezing, $\Delta t_{melting}$ is the amount of time spent melting, and $\Delta t_{changeover}$ is the amount of time spent changing the system over from freezing to

melting. The value of $\Delta t_{changeover}$ was held at a constant 20 minutes, broken up into 10 minutes after the freezing stage and 10 minutes after the melting stage. The melting time $\Delta t_{melting}$ is dependent on the freezing because the melting cycle must be run until all ice has been melted. Thus, the volume production over time of the entire system can be studied by varying $\Delta t_{freezing}$ only.

To investigate the behavior of the full system, the freezing spacial-temporal analysis conducted by Whitaker [6] was run for times in the range of 50 - 6000 seconds and the resulting volume of ice was recorded. The melting second order analysis was then run until it completely melted that volume of ice. When combined, these analyses give the times for freezing and melting, as well as the volumes produced at each stage. By adding the run time of the freezing cycle, melting cycle, and the changeover time, the full cycle length was calculated for each run. The volume of water per day was calculated by multiplying the output volume of each different cycle length by the number of cycles that could be run per day. Figure 16 shows the volume per day that can be produced versus cycle time. This figure reports the output of only one pipe. In practice many pipes would be used together as part of one heat exchanger.

The maximum amount of product water per day is 12.3 liters. This is the output of only one tube. Tubes will be assembled in arrays of twenty five, which would constitute one heat exchanger. Each heat exchanger would be capable of producing 307.5 liters per day. To achieve this amount the system should run at a cycle time of 68.2 minutes. This is made up of 17.2 minutes of freezing, 10 min-

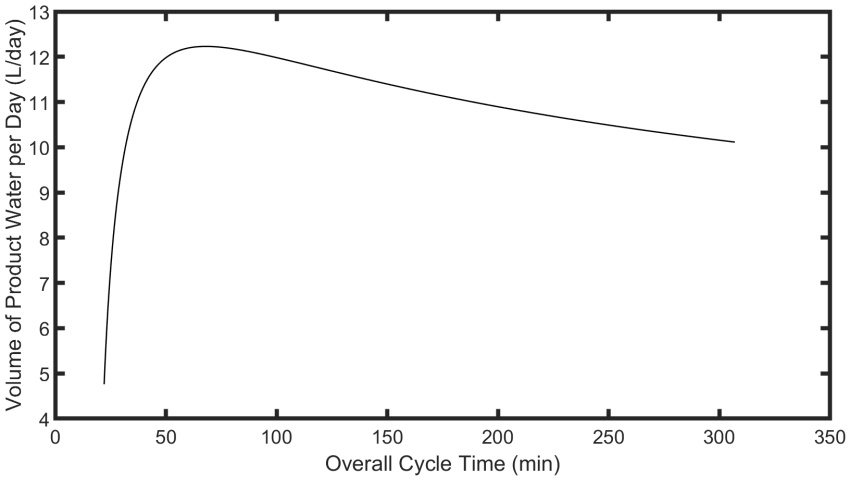

Figure 16: Cycle Time τ_{cycle} versus Product Water per Day

utes of changeover, 31 minutes of melting, and another 10 minutes of changeover. However, for $45 < \tau_{cycle} < 100$ minutes there is very little change in the overall product water volume, so for a real application the user could operate anywhere inside these bounds with little effect on productivity. Operating on the higher side of this range would necessitate spacing the pipes out farther from each other in the heat exchanger to avoid influencing one another, which was not considered in the analysis.

The run times for freezing and melting show that freezing is nearly twice as fast as melting. This is because the changing thermal resistance for freezing uses the thermal conductivity of ice, which conducts heat better than water. Improvements to the melting cycle would be the most beneficial because it is the slowest of any operation.

Using Equations 27 and 28 the power requirement of the pump can be calculated. First, the Darcy friction factor must be estimated. Using the mass flow rate

at the base case and the dynamic viscosity at the inlet temperature the Reynolds number is 16535 indicating a fully turbulent flow. Using the Moody chart and a relative roughness of 0.025 for a steel pipe, the Darcy friction factor is approximately 0.56. Using this value in Equations 27 and 28 the pump power is 112 watts. This amounts to 161.3 kWh per day. The power of a chiller used for freezing is 6 kW which is 36.3 kWh per day. The heating will mostly be done by ambient temperature, but to look at the worst case the heater power requirements will be set equal to the chiller requirements. This results in a system-wide energy requirement of 234 kWh per day. Because this much power produces 12.3 L, each liter of water requires 19 kWh of energy.

5 CONCLUSIONS

Three models were developed to approximate the behavior of the melting cycle for a freeze-thaw desalination system. The zeroth order analysis treats the system as steady state to show the maximum output for an ideal case. The first order analysis accounts for variations in time to capture the effect of an increasing thermal resistance due to melted water. The second order analysis allows variation axially along the length of the system to better model the effect of the working fluid's varying temperature. The changing resistance of the melted water in the first and second order analyses was described in three ways; conduction through water, conduction through ice, and natural convection. The natural convection produced complex numbers due to water's negative thermal expansion coefficient values for water near the temperature of phase change. Of the other two, conduction through water produced less water so it was used as the more conservative case.

The three analyses used a base case as a starting point to output realistic numbers. The base case consisted of a mass flow rate of 0.1 kg/s, working fluid temperature inlet of 293 K, pipe inner radius of 3.85 mm, and pipe outer radius of 4.95 mm. The influence of these variables on the output of the system was investigated. An increase of each of the variables except radii resulted in an increase of output volume from the system. An increase in radii did increase the volume of product water, but only true for the case of a single pipe. When

comparing volumes using the number of pipes in a 100cm x 100cm area, the smaller radii were preferable. This was due to the increased surface area for a larger number of the smaller pipes. The length of the pipe had a positive linear relationship with both pump power required and volume of product water. An increase in the mass flow rate increased the volume output, but there was no benefit using values above 0.1 kg/s. The working fluid inlet temperature had a positive relationship with volume output. This effect was more pronounced when the inlet temperature was close to the phase change temperature.

When the second order melting analysis was used in conjunction with a similar freezing analysis, the overall freeze desalination cycle was examined. A model was developed which ran a freezing stage, 10 minutes of changeover, a melting stage, and another 10 minutes of changeover. The cycle lengths which produced the most product water per day were 17.2 minutes of freezing and 31 minutes of melting, resulting in an overall cycle time of 68.2 minutes. The setup produced 12.3 liters per day per tube. For a typical heat exchanger design using an array of 25 tubes this creates 307.5 liters per day for each heat exchanger. Each liter of water requires 22.5 kWh of energy for the system.

6 RECOMMENDATIONS

To improve on the melting analysis model natural convection should be incorporated in some way. Natural convection in the system would reduce the resistance of the melted water and increase the output of the system. This was attempted in the analysis but rejected due to the negative thermal expansion coefficient causing problems with the Rayleigh number. Even though the equations don't give reasonable answers there will still be natural convection in the system due to density variations of the water. Developing a different method for calculating the Rayleigh number that allows negative thermal expansion coefficients would allow these analyses to become much more accurate and representative of the expected behavior of the system. Finding a way to make this model work could be investigated as well, such as attempting to use the absolute value of the thermal expansion coefficient or using only the real part of the effective thermal conductivity. If this route is pursued caution should be exercised as it may not give the intended results.

The in-depth analysis reveals the strengths and weaknesses of the proposed freeze desalination system. For these analyses it was assumed that every bit of desalination was accomplished by a running system. However, this does not have to be the case. Through mechanical design it could be possible to drastically decrease the melting cycle time. If it was possible to melt only the innermost millimeter of ice and then mechanically remove the rest, the ice could be melted in a different container by the ambient temperature or a small heater. This would

cut the melting cycle length from 31 minutes to less than 2 minutes. Keeping the freeze cycle and changeover times the same, this would boost the output from 12.3 liters per day to 21.3 liters per day.

The biggest long-term issue for this system is the same for all methods of desalination - how to dispose of the excess salt and contaminants. This salt can be repurposed for uses such as de-icing road salt, but it is most commonly put back in a body of water that eventually runs to an ocean. This excess salt can be devastating to marine life [20]. Millions of cubic meters of brine are created each day by desalination plants around the world. Until a solution can be reached for brine disposal, desalination has a serious drawback that should be avoided whenever possible.

REFERENCES

[1] I. A. Shiklomanov. World fresh water resources. *Water in Crisis*, 1:13–24, 1993.

[2] A. Cardona, J. Carrillo-Rivera, R. Huizar-Alvarez, and E. Graniel-Castro. Salinization in coastal aquifers of arid zones: an example from santo domingo, baja california sur, mexico. *Environmental Geology*, 45:350–366, 2004.

[3] R. Prince. Salt (sodium chloride) in drinking water. 2016. URL: `https://ww2.health.wa.gov.au/Articles/S_T/Sodium-in-drinking-water` (visited on 02/15/2019).

[4] T. Mills, P. Hoekstra, M. Blohm, and L. Evans. Time domain electromagnetic soundings for mapping sea-water intrusion in monterey county, california. *Ground Water*, 26:350–366, 1988.

[5] L. Bernstein. Salt tolerance of fruit crops. *Agricultural Research Service*, 292:3, 1965.

[6] T. Whitaker. Freeze stage analysis of an indirect freeze desalination system. *UHC Thesis, Oregon State University*, 2019.

[7] P. G. Youssef, R. K. Al-Dadah, and S. M. Mahmoud. A comparative analysis of desalination technologies. *Energy Procedia*, 61:2604–2607, 2014.

[8] L. F. Greenlee, D. F. Lawler, B. D. Freeman, B. Marrot, and P. Moulin. Reverse osmosis desalination: water sources, technology,and today's challenges. *Water Research*, 43:2317–2348, 2009.

[9] J. E. Miller. *Review of Water Resources and Desalination Technologies*. Sandia National Laboratories, 2003.

[10] M. Sadrzadeh and T. Mohammadi. Sea water desalination using electrodialysis. *Desalination*, 221:440–447, 2008.

[11] A. D. Khawajia, I. K. Kutubkhanaha, and J.-M. Wieb. Advances in seawater desalination technologies. *Desalination*, 221:47–69, 2008.

[12] A. A. Attia. New proposed system for freeze water desalination using auto reversed r-22 vaporcompression heat pump. *Desalination*, 254:179–184, 2010.

[13] Z. Lu and L. Xu. Freezing desalination process. *Encyclopedia of Desalination and Water Resources*, 2, 2013.

[14] G. Nebbia and G. N. Menozzi. Early experiments on water desalination by freezing. *Desalination*, 5:49–54, 1968.

[15] M. Rahman, M. Ahmed, and X. Chen. Freeze-melting process and desalination: review of the state-of-the-art. *Sep. Purif. Rev.*, 35:59–96, 2006.

[16] P. Wang and T.-S. Chung. A conceptual demonstration of freeze desalination–membrane distillation (fd–md) hybrid desalination process utilizing liquefied natural gas (lng) cold energy. *Water Research*, 47:4037–4052, 2012.

[17] R. Fujioka, L. Wang, G. Dodbiba, and T. Fujita. Application of progressive freeze-concentration for desalination. *Desalination*, 319:33–37, 2013.

[18] F. Boschetti. Reliability analysis of a freeze desalination system. *UHC Thesis, Oregon State University*, 2019.

[19] T. L. Bergman, A. S. Lavine, F. P. Incropera, and D. P. Dewitt. *Fundamentals of Heat and Mass Transfer*. John Wiley & Sons Inc., 2011. Massachusetts.

[20] C. Fortuna. Humans worth their salt? the price of desalination = brine disposal. 2019. URL: `https://cleantechnica.com/2019/01/17/humans-worth-their-salt-the-price-of-desalination-brine-disposal/` (visited on 01/17/2019).

APPENDICES

Appendix A - Zeroth Order Code

```
function [timevector,Volume] = analysis_zero_order(
   Twf_in,Twf_out,mwf_dot,finaltime,deltat)
%UNTITLED Summary of this function goes here

rho_w = 1000;              %kg/m^3
lambda_w = 330000;         %J/kg
Cwf = 4220;                %J/kg-K

timevector = 0:deltat:finaltime;

Qdot = mwf_dot * Cwf * (Twf_out - Twf_in);
%Qdot = -576.8384;

Volume_meters3 = -Qdot / (rho_w * lambda_w) * timevector
   ;
Volume = 1000 * Volume_meters3;

end
```

Appendix B - First Order Code

```
function [time,Volume,Twf_out_avg] =
   analysis_first_order(L,rA,rB,mwf_dot,finaltime,Twf_in
   ,deltat)
%first_func executes first order analysis

%Setting deltat step size and the size of rC
rC = zeros(1,finaltime/deltat);
time = 0:deltat:finaltime;

%Working Fluid Properties
h_wf = 4000;                          %PLACEHOLDER. NEED
   ACTUAL VALUE OF REFRIGERANT
Cwf = 4220;                           %Specific heat of
   water at 1atm, 274 K (J/kg-K)
rho_wf = 1000;                        %Working Fluid
   density (kg/m^3)
mwf = pi * rA.^2 * L * rho_wf;        %Mass of working
   fluid in pipe (kg)

%Water/ice properties
lambda_sf = 330000;                   %Enthalpy phase
   change for water/ice (J/kg)
rho_w = 1000;                         %Density of water (kg
   /m^3)
k_w = 0.55575;                        %Thermal conductivity
    at 273.5 K liquid water (W/m-K)
k_I = 2.25;                           %Thermal conductivity
    of ice (W/m-K)
k_p = 17;                             %Thermal conductivity
    of stainless steel pipe (W/m-K)
T_pc = 273.15;                        %Temp of phase change
    (K)


%Thermal resistance calculations
R_wf = 1/(2 * pi * rA * L * h_wf); %Thermal resistance
   of refrigerant (K/W)
R_P = log(rB/rA)/(2*pi*k_p*L);        %Thermal resistance
   of pipe (K/W)

%Create vectors of correct size for unknowns
R_W = zeros(1,length(rC));
```

```
Twf_out = zeros(1,length(rC));
Twf_avg = zeros(1,length(rC));
Qdot = zeros(1,length(rC));

%Set initial conditions
rC(1) = rB+0.00001;

i = 1;

%Loop solves R_W, then matrices, then k_eff, then
   repeats
while time(i) < finaltime

    %Calculates resistance of water using most current
       k_eff & rC
    R_W(i) = log(rC(i) / rB)/(2*pi*k_w*L);
    R_sum = R_W(i) + R_P + R_wf;

    %For the first iteration there is no Twf_avg(i-1) so
        that term is
    %removed and calculated separately
    if i == 1
        M1 = [mwf_dot * Cwf * Twf_in;
              T_pc / R_sum;
              Twf_in;
              lambda_sf * rho_w * pi * L * (rC(i) .^2)];

        M2 = [-1, 0, mwf_dot * Cwf, 0;
              1, 1/R_sum, 0, 0;
              0, 2, -1, 0;
              deltat, 0, 0, lambda_sf * rho_w * pi * L *
                 rC(i)];


    else
              M1 = [mwf_dot * Cwf * Twf_in + mwf * Cwf /
                 deltat * Twf_avg(i-1);
              T_pc / R_sum;
              Twf_in;
              lambda_sf * rho_w * pi * L * (rC(i) .^2)];

              M2 = [-1, mwf * Cwf / deltat, mwf_dot * Cwf,
                  0;
              1, 1/R_sum, 0, 0;
```

```
            0, 2, -1, 0;
            deltat, 0, 0, lambda_sf * rho_w * pi * L *
               rC(i)];

    end
    M3 = M2 \ M1;
    Qdot(i) = M3(1);
    Twf_avg(i) = M3(2);
    Twf_out(i) = M3(3);
    rC(i+1) = M3(4);

    %time(i+1) = deltat + time(i);

    i = i + 1;

end

Volume = (rC.^2 - rB.^2)*pi*L * 1000;
Twf_out_avg = mean(Twf_out(1:1000));


tempend = [Twf_in Twf_out(end)];
tempmid = [Twf_in Twf_out(finaltime./deltat/10)];
lengthvec = [0 L];
figure(2)
hold on
plot(lengthvec, tempend, ':k','LineWidth',2)
figure(3)
plot(lengthvec, tempmid, ':k','LineWidth',2)
end
```

Appendix C - Second Order Code

```
function [time,Volume,rC,Qdot] = analysis_second_order(L
    ,rA,rB,mwf_dot,finaltime,T_initial,deltat)
%UNTITLED4 Summary of this function goes here
%   Detailed explanation goes here

hold on

%Setting delta time and space values
deltaz = L / 50;                                        %
    Meters between each space step
num_timesteps = finaltime/deltat;
num_spacesteps = L / deltaz;
time = 0:deltat:finaltime;

%Refrigerant properties
%Ethylene Glycol as working fluid
%h_wf = 550; %PLACEHOLDER. NEED ACTUAL VALUE OF
    REFRIGERANT
%Cwf = 3627; %Specific heat of ethylene glycol at 10 deg
    C. (J/kg*C)
%rho_wf = 1047;
%Water as working fluid

h_wf = 4000;
Cwf = 4220;
rho_wf = 1000;
mwf = pi * rA.^2 * L * rho_wf;
mwf_step = pi * rA.^2 * deltaz * rho_wf;
lengthvect = 0:deltaz:L;

%Water/ice properties
lambda_sf = 330000;                                     %
    Enthalpy phase change for water/ice (J/kg)
rho_water = 1000;                                       %Density
    of water (kg/m^3)
k_w = 0.55575;                                          %Thermal
    conductivity at 0.1 degC liquid water (W/m-K)
k_I = 2.25;                                             %Thermal
    conductivity of ice (W/m-C)
k_p = 61;                                               %Thermal
    conductivity of copper pipe (W/m-K)
```

```
T_pc = 273.15;                                          %Temp
   of phase change (K)

%Resistance Calculations
R_wf = 1/(2 * pi * rA * L * h_wf);                       %
   Thermal resistance of refrigerant (deg. C/W)
R_wf_step = 1/(2 * pi * rA * deltaz * h_wf);
R_P = log(rB/rA)/(2*pi*k_p*L);                          %Thermal
    resistance of pipe (deg. C/W)
R_P_step = log(rB/rA)/(2*pi*k_p*deltaz);                %m^2-k/W


%Size unknowns for simultaneous equations
Twf_out = zeros(num_timesteps,num_spacesteps);
Twf_avg = zeros(num_timesteps,num_spacesteps);
Qdot = zeros(num_timesteps,num_spacesteps);
Twf_in = zeros(num_timesteps,num_spacesteps);
R_W = zeros(num_timesteps,num_spacesteps);
rC = zeros(num_timesteps,num_spacesteps);
R_sum = zeros(num_timesteps,num_spacesteps);


%Set initial conditions
rC(1,:) = rB + 0.00001;
                                          %Outer radius of ice
   (m)
Twf_in(:,1) = T_initial;
                                           %Working Fluid temp
    (deg. C)
i = 1;

while time(i) < finaltime
    for j = 1:num_spacesteps
        %Newest Resistance through water using k_I
        R_W(i,j) = log(rC(i,j) / rB)/(2 * pi * k_w *
           deltaz);
        R_sum(i,j) = R_P_step + R_wf_step + R_W(i,j);


        %Matrix Math
        if i == 1

            M1 = [mwf_dot * Cwf * Twf_in(i,j);
                T_pc / R_sum(i,j);
```

```
                Twf_in(i,j);
                lambda_sf * rho_water * pi * deltaz * (
                   rC(i,j) .^2)];


            M2 = [-1, 0, mwf_dot * Cwf, 0;
                1, 1/R_sum(i,j), 0, 0;
                0, 2, -1, 0;
                deltat, 0, 0, lambda_sf * rho_water * pi
                    * deltaz * rC(i,j)];

        else

            M1 = [mwf_dot * Cwf * Twf_in(i,j) + mwf_step
                * Cwf / deltat * Twf_avg(i-1,j);
                T_pc / R_sum(i,j);
                Twf_in(i,j);
                lambda_sf * rho_water * pi * deltaz * (
                   rC(i,j) .^2)];

            M2 = [-1, mwf_step * Cwf / deltat, mwf_dot *
                Cwf, 0;
                1, 1/R_sum(i,j), 0, 0;
                0, 2, -1, 0;
                deltat, 0, 0, lambda_sf * rho_water * pi
                    * deltaz * rC(i,j)];
        end

        M3 = M2 \ M1;
        Qdot(i,j) = M3(1);
        Twf_avg(i,j) = M3(2);
        Twf_out(i,j) = M3(3);
        rC(i+1,j) = M3(4);

        %Outlet temp of this cell is inlet temp of next
           cell
        if j ~= num_spacesteps
            Twf_in(i,j+1) = Twf_out(i,j);
        end

    end

    i = i + 1;
end
```

```
Volume = 1000 * pi * deltaz .* (rC.^2 - rB.^2);

A = 0.5 * pi .* rC.^2;
velo = mwf_dot ./ (A * rho_water);

T_overall = [Twf_in(:,1) Twf_out];

figure(2)

hold on
plot(lengthvect,T_overall(end,:),'--k','LineWidth',2)
xlabel('Axial Position (m)')
ylabel('Working Fluid Temperature (deg. K)')
ax = gca;
ax.XRuler.Exponent = 0;
set(gca,'FontSize',24,'LineWidth',6)
legend('First Order Temp. Profile','Second Order Temp.
   Profile','Location','northeast')

figure(3)
plot(lengthvect,T_overall(finaltime./deltat./10,:),'--k'
   ,'LineWidth',2)
xlabel('Axial Position (m)')
ylabel('Working Fluid Temperature (deg. K)')
ax = gca;
ax.XRuler.Exponent = 0;
set(gca,'FontSize',24,'LineWidth',6)
legend('First Order Temp. Profile','Second Order Temp.
   Profile','Location','northeast')
end
```